

A peer-reviewed version of this preprint was published in PeerJ on 30 April 2019.

[View the peer-reviewed version](https://peerj.com/articles/6845) (peerj.com/articles/6845), which is the preferred citable publication unless you specifically need to cite this preprint.

Khider M, Hansen H, Hjerde E, Johansen JA, Willassen NP. 2019.

Exploring the transcriptome of *luxI*⁻ and *ΔainS* mutants and the impact of N-3-oxo-hexanoyl-L- and N-3-hydroxy-decanoyl-L-homoserine lactones on biofilm formation in *Aliivibrio salmonicida*. PeerJ 7:e6845

<https://doi.org/10.7717/peerj.6845>

Exploring the transcriptome of *luxI* and Δ *ainS* mutants and the impact of N-3-oxo-hexanoyl-L- and N-3-hydroxy-decanoyl-L-homoserine lactones on biofilm formation in *Aliivibrio salmonicida*

Miriam Khider ^{Corresp., 1}, Hilde Hansen ¹, Jostein A. Johansen ², Erik Hjerde ^{1,3}, Nils Peder Willassen ^{1,3}

¹ Norwegian Structural Biology Centre, Department of Chemistry, Faculty of Science and Technology, UiT-The Arctic University of Norway, N-9037 Tromsø, Norway

² Department of Chemistry, Faculty of Science and Technology, UiT-The Arctic University of Norway, N-9037 Tromsø, Norway

³ Centre for bioinformatics, Department of Chemistry, Faculty of Science and Technology, UiT - The Arctic University of Norway, N-9037 Tromsø, Norway

Corresponding Author: Miriam Khider
Email address: miriam.khider@uit.no

Background. The marine bacterium *A. salmonicida* uses the quorum sensing (QS) systems, AinS/R and LuxI/R to produce eight acyl-homoserine lactones (AHLs) in a cell density dependent manner. Biofilm formation is one of the QS regulated phenotypes, which requires the expression of exopolysaccharides (EPS). We previously demonstrated that inactivation of LitR, the master regulator of QS in *A. salmonicida* resulted in biofilm formation, which was, similar to the biofilm formed by the AHL deficient mutant Δ *ainSluxI*. In this work, we have identified genes regulated by AinS and LuxI using RNA sequencing (RNA-Seq), and studied their role in biofilm formation, colony morphology and motility. We have also studied the effect of two AHLs on the biofilm formation.

Results. The transcriptome profiling of Δ *ainS* and *luxI* mutants allowed us to identify essential genes regulated by QS in *A. salmonicida*. Relative to the wild-type, the Δ *ainS* and *luxI* mutants revealed 40 and 500 differentially expressed genes (DEGs), respectively. The functional analysis demonstrated that the most pronounced DEGs were involved in bacterial motility and chemotaxis, exopolysaccharide production, and surface structures related to adhesion. Inactivation of *luxI* but not *ainS* genes resulted in wrinkled colony morphology. While inactivation of both genes (Δ *ainSluxI*) resulted in strains able to form wrinkled colonies and mushroom structured biofilm. Moreover, when the Δ *ainSluxI* mutant was supplemented with N-3-oxo-hexanoyl-L-homoserine lactone (3OC6-HSL) and N-3-hydroxy-decanoyl-L-homoserine lactone (3OHC10-HSL), the biofilm did not develop. We also show that LuxI is needed for motility and repression for EPS production, where repression of EPS is likely operated through the RpoQ-sigma factor.

Conclusion. These findings imply that LuxI and AinS synthases have a critical contribution to the QS-dependent regulation on gene expression and the phenotypic traits related to it.

1 **Exploring the transcriptome of *luxI* and *ΔainS* mutants and the impact of N-**
2 **3-oxo-hexanoyl-L- and N-3-hydroxy-decanoyl-L-homoserine lactones on**
3 **biofilm formation in *Aliivibrio salmonicida***

4 Miriam Khider¹, Hilde Hansen¹, Jostein A. Johansen¹, Erik Hjerde^{1,2} and Nils Peder Willassen^{1,2}

5 ¹Norwegian Structural Biology Centre, Department of Chemistry, Faculty of Science and
6 Technology, UiT - The Arctic University of Norway, N-9037 Tromsø, Norway

7 ²Centre for bioinformatics, Department of Chemistry, Faculty of Science and Technology, UiT -
8 The Arctic University of Norway, N-9037 Tromsø, Norway

9 Corresponding Authors:

10 Miriam Khider

11 UiT - The Arctic University of Norway, N-9037 Tromsø, Norway

12 Email address: miriam.khider@uit.no

13 Nils Peder Willassen

14 Email address: nils-peder.willassen@uit.no

15 UiT - The Arctic University of Norway, N-9037 Tromsø, Norway

16 **Abstract**

17 **Background.** The marine bacterium *A. salmonicida* uses the quorum sensing (QS) systems,
18 AinS/R and LuxI/R to produce eight acyl-homoserine lactones (AHLs) in a cell density
19 dependent manner. Biofilm formation is one of the QS regulated phenotypes, which requires the
20 expression of exopolysaccharides (EPS). We previously demonstrated that inactivation of LitR,
21 the master regulator of QS in *A. salmonicida* resulted in biofilm formation, which was, similar to
22 the biofilm formed by the AHL deficient mutant $\Delta ainSluxI$. In this work, we have identified
23 genes regulated by AinS and LuxI using RNA sequencing (RNA-Seq), and studied their role in
24 biofilm formation, colony morphology and motility. We have also studied the effect of two
25 AHLs on the biofilm formation.

26 **Results.** The transcriptome profiling of $\Delta ainS$ and *luxI* mutants allowed us to identify essential
27 genes regulated by QS in *A. salmonicida*. Relative to the wild-type, the $\Delta ainS$ and *luxI* mutants
28 revealed 40 and 500 differentially expressed genes (DEGs), respectively. The functional analysis
29 demonstrated that the most pronounced DEGs were involved in bacterial motility and
30 chemotaxis, exopolysaccharide production, and surface structures related to adhesion.
31 Inactivation of *luxI* but not *ainS* genes resulted in wrinkled colony morphology. While
32 inactivation of both genes ($\Delta ainSluxI$) resulted in strains able to form wrinkled colonies and
33 mushroom structured biofilm. Moreover, when the $\Delta ainSluxI$ mutant was supplemented with N-
34 3-oxo-hexanoyl-L- homoserine lactone (3OC6-HSL) and N-3-hydroxy-decanoyl-L-homoserine
35 lactone (3OHC10-HSL), the biofilm did not develop. We also show that LuxI is needed for

36 motility and repression for EPS production, where repression of EPS is likely operated through
37 the RpoQ-sigma factor.

38 **Conclusion.** These findings imply that LuxI and AinS synthases have a critical contribution to
39 the QS-dependent regulation on gene expression and the phenotypic traits related to it.

40 **Introduction**

41 Quorum sensing (QS) is a widespread mechanism in bacteria, which employs autoinducing
42 chemical signals in response to cell density to coordinate several traits as biofilm formation,
43 motility, bioluminescence and virulence (Whitehead et al., 2001). A variety of classes of QS
44 chemical signals have been identified in different bacteria. Gram-negative bacteria usually
45 employ N-acyl homoserine lactones (AHLs) which contain a conserved homoserine lactone
46 (HSL) ring and an amide (N)-linked acyl side chain. The acyl groups identified to date, range
47 from 4 to 18 carbons in length (Fuqua, Parsek, & Greenberg, 2001; Swift et al., 2001; Whitehead
48 et al., 2001). AHL-mediated QS was originally discovered in the marine bacterium *Aliivibrio*
49 (*vibrio*) *fischeri*, which was found to regulate bioluminescence in a cell-density dependent
50 manner (Eberhard et al., 1981; Ruby & Lee, 1998). *A. fischeri* controls luminescence by the QS
51 systems LuxS/LuxPQ, LuxI/LuxR and AinS/AinR, where LuxS, LuxI and AinS are the
52 autoinducer synthases (Lupp & Ruby, 2005, 2004; Lupp et al., 2003). LuxI synthesizes a
53 diffusible molecule, N-(3-oxohexanoyl)-L-homoserine lactone (3OC6-HSL), which increases in
54 concentration with cell density. 3OC6-HSL then binds to LuxR, and this complex activate light
55 production from *lux* operon (Verma & Miyashiro, 2013).

56 The marine bacterium *Aliivibrio salmonicida*, is known to cause cold-water vibriosis in Atlantic
57 salmon (*Salmo salar*), rainbow trout (*Oncorhynchus mykiss*) and captive Atlantic cod (*Gadus*
58 *morhua*) (Egidius et al., 1981; Egidius et al., 1986; Holm et al., 1985). The genome sequence of
59 *A. salmonicida* revealed five QS systems, where three are similar to those of *A. fischeri*, the
60 LuxS/PQ, LuxI/P and AinS/R (Hjerde et al., 2008). *A. salmonicida* produces eight AHLs, where
61 the LuxI/R system is responsible for seven AHLs (3OC4-HSL, C4-HSL, 3OC6-HSL, C6-HSL,
62 C8-HSL, 3OC8-HSL and 3OC10-HSL) while the AinS/R system synthesizes only one
63 autoinducer, 3OHC10-HSL (Hansen et al., 2015). Although, *A. salmonicida* encodes the *lux*
64 operon (*luxCDABEG*) (Nelson et al., 2007), the bacteria is only able to produce bioluminescence
65 after addition of decyl aldehyde (Fidopiastis, Sørum & Ruby, 1999). LitR, the master regulator
66 of QS is a positive regulator of AHL production and hence, cryptic bioluminescence in *A.*
67 *salmonicida* (Bjelland et al., 2012).

68 In addition to regulating bioluminescence, AHLs are also involved in multiple other
69 physiological processes in bacteria such as production of virulence factors, drug resistance and
70 biofilm formation (Abisado et al., 2018). AHL-mediated QS affects biofilm formation in a
71 number of bacterial species (Fazli et al., 2014; Yildiz & Visick 2009; Hmelo, 2017), and is
72 associated with almost all stages, such as initial surface attachment, bacterial growth, maturation,
73 and detachment of cells. For some species, QS regulates flagellar activity, which in turn
74 influences the attachment of bacteria to surface (Guvener & McCarter 2003; Pratt & Kolter
75 1998). In *Pseudomonas aeruginosa* PAO1 and *Burkholderia cepacia*, QS regulates other
76 aspects of biofilm formation, including biofilm structure and maturation (Huber et al., 2001;
77 Whitehead et al., 2001). QS further increases dispersal of detached bacteria from mature biofilm
78 to trigger a new cycle of biofilm formation (Emerenini et al., 2015). In many *Vibrio* species

79 development of rugose colony morphology and biofilm formation correlates with
80 exopolysaccharide production. For example, in *Vibrio parahaemolyticus* and *Vibrio vulnificus*,
81 QS activate formation of biofilm and opaque colonies at high cell density. Mutation in the QS
82 regulators OpaR and SmcR in *V. parahaemolyticus* and *V. vulnificus*, respectively results in
83 translucent colonies indicating a decrease in exopolysaccharide production (Lee et al., 2013;
84 McCarter, 1998). In contrast to the two species mentioned above, *Vibrio cholerae* presents a
85 different effect of QS regulation on biofilm formation. A mutation in the master regulator HapR,
86 results in a state mimicking low cell density conditions, where the mutant produces more
87 exopolysaccharides compared to wild-type (Zhu & Mekalanos, 2003). *A. salmonicida* behaves in
88 a similar fashion to *V. cholerae*, where deletion of *litR* leads to increase exopolysaccharide
89 production and formation of three-dimensional biofilm structure (Bjelland et al., 2012; Hansen et
90 al., 2014).

91 We have previously shown that AinS and LuxI in *A. salmonicida* are responsible for the
92 production of eight AHLs and that both these AHL synthases are needed for downregulation of
93 biofilm formation (Hansen et al., 2015). In the work presented here, we show that the AHLs
94 3OC6-HSL (LuxI product) and 3OHC10-HSL (AinS product) are biologically active and
95 downregulate biofilm formation in *A. salmonicida*. RNA-Seq was performed to identify genes
96 regulated by AinS/R and LuxI/R QS systems. At high cell density, inactivation of *luxI* had a
97 global effect on the transcriptome and resulted in nearly 500 differently expressed genes (DEGs),
98 whereas deletion of *ainS* only resulted in 29 DEGs at the same condition. Genes involved in
99 motility and EPS production were among the DEGs in the *luxI* mutant, which explains the
100 finding that this mutant lacks flagella, is non-motile and produces rugose colonies.

101 **Materials and methods**

102 **Bacterial strains, culture conditions and supplements**

103 Bacterial strains used in this study are listed in Table 1. *A. salmonicida* LFI1238 strain and the
104 *A. salmonicida* mutants were grown from a frozen glycerol stock on blood agar base no. 2
105 (oxid, Cambridge, UK) with a total concentration of 5% blood and 2.5% NaCl (BA2.5) or in
106 Luria Berthani broth (Difco, BD Diagnostics, Sparks, MD) with a total concentration of 2.5%
107 NaCl (LB2.5). *A. salmonicida* strains were cultivated from a single colony in 2 ml (LB2.5) at
108 12°C, 220 rpm for 2 days (primary culture). The primary cultures were diluted 1:20 and grown at
109 12°C, 220 rpm for an additional day (secondary cultures).

110 The GFP (green fluorescence protein) constitutive plasmid pVSV102 and helper plasmid
111 pEVS104 propagated in *Escherichia coli* (*E. coli*), DH5 α pir and CC118 λ pir, respectively. The
112 *E. coli* strains were cultivated in LB or LA containing 1% NaCl (LB1 and LA1 respectively) and
113 incubated at 12°C and 220 rpm. The potential tagged strains were selected on BA2.5
114 supplemented 150 μ l/ml kanamycin.

115 A seawater-based medium (SWT) was used for the HPLC-MS/MS, transcriptomics, biofilm and
116 morphology assay. The medium consists of 5 g/L of bacto peptone (BD), 3 g/L of yeast extract
117 (Sigma) and 28 g/L of a synthetic sea salt (Instant Ocean, Aquarium Systems).

118 **Transcriptomics**

119 *Sample collection*

120 Three biological replicates were used for *A. salmonicida* LFI1238 wild-type
121 strains. The overnight secondary cultures were diluted to $OD_{600} = 0.05$ (optical density measured
122 at 600 nm) in a total volume of 70 ml SWT media supplemented with 2.5% sea salt. The cultures
123 were grown further at 8°C and 220 rpm in 250 ml baffled flask. Samples (10 ml) at low cell
124 density $OD_{600} = 0.30$ and (2.5 ml) at high cell density $OD_{600} = 1.20$ were harvested (13000 x g,
125 2 minutes, 4°C) (Heraeus 3XR, Thermo Scientific). Samples were preserved in *RNAlater* and
126 stored at -80°C until RNA extraction.

127 *Total RNA isolation and rRNA depletion*

128 The total RNA was extracted from the cell pellets following the standard protocols by
129 manufactures (Masterpure DNA & RNA purification kit, Epicenter). The quality of total RNA
130 was determined using a Bioanalyzer and Total RNA nano chip (Agilent Technologies). The
131 ribosomal rRNA was removed from the samples using Ribo-Zero rRNA Removal kit for bacteria
132 (Illumina) following manufactures instructions. The quality of RNA after depletion was
133 determined using Bioanalyzer and Total RNA pico chip (Agilent Technologies).

134 *RNA sequencing and data analysis*

135 The rRNA depleted samples were used to generate RNA-sequencing libraries using TruSeq
136 strandand mRNA library prep kit (Illumina), and sequenced at the Norwegian Sequencing Center

137 using the Illumina NextSeq 500 with mid output reagents with 75 bp. read length and paired end
138 reads.

139 The sequencing quality of FASTQ files was assessed using FastQC (Available online at:
140 <http://www.bioinformatics.babraham.ac.uk/projects/fastqc>). Further analysis of the RNA-Seq
141 data was performed using EDGE-pro v1.0.1 (Magoc, Wood, & Salzberg, 2013) and DESeq2
142 (Love, Huber & Anders, 2014). EDGE-pro was used to align the reads to the *A. salmonicida*
143 LFI1238 genome (Hjerde et al., 2008), and to estimate gene expression levels. Differences in
144 gene expression between wild-type and $\Delta litR$ and $\Delta rpoQ$ mutants were determined using
145 DESeq2. Log2 fold changes of the genes were recalculated to \times differential expression values
146 (i.e., $\Delta ainS/wt$) and genes were defined as significantly differentially expressed genes based on a
147 p-value ≤ 0.05 and differentially expression values (fold change values) of $\geq 2 \times$ and $\leq -2 \times$.
148 tRNA and rRNA reads were filtered out before analysis.

149 The sequences of $\Delta ainS$, *luxI* and *A. salmonicida* LFI1238 have been deposited in the European
150 Nucleotide Archive (www.ebi.ac.uk/ena) under study accession numbers PRJEB29457 and
151 PRJEB28385, respectively.

152 **High-Performance Liquid Chromatography Tandem Mass Spectrometry (HPL-MS/MS)**
153 **assay**

154 *AHL standards*

155 AHL standards purchased from University of Nottingham, UK were: N-3-oxo-butyryl-L-
156 homoserine lactone (3OC4-HSL), N-3-hydroxy-butyryl-L-homoserine lactone (3OHC4-HSL),
157 N-3-hydroxy-hexanoyl-L-homoserine lactone (3OHC6-HSL), N-3-hydroxy-octanoyl-L-
158 homoserine lactone (3OHC8-HSL), N-3-hydroxy-decanoyl-L-homoserine lactone (3OHC10-
159 HSL). Standards purchased from Sigma-Aldrich were: N-butyryl-DL-homoserine lactone (C4-
160 HSL), N-hexanoyl-L-homoserine lactone (C6-HSL), N-3-oxo-hexanoyl-L-homoserine lactone
161 (3OC6-HSL), N-octanoyl-L-homoserine lactone (C8-HSL), N-3-oxo-octanoyl-L-homoserine
162 lactone (3OC8-HSL), N-decanoyl-DL-homoserine lactone (C10-HSL), N-3-oxo-decanoyl-L-
163 homoserine lactone (3OC10-HSL), N-dodecanoyl-DL-homoserine lactone (C12-HSL), N-3-oxo-
164 dodecanoyl-L-homoserine lactone (3OC12-HSL), and N-3-hydroxy-dodecanoyl-DL-homoserine
165 lactone (3OHC12-HSL). Acetonitrile and formic acid for HPLC were purchased from Sigma.

166 *Preparation of bacterial supernatants for AHL measurements*

167 Two biological replicates were used for all *A. salmonicida* strains. The overnight secondary
168 cultures were diluted to an $OD_{600} = 0.05$ in a total volume of 60 ml SWT media supplemented
169 with 2.5% sea salt. The cultures were grown further at 8°C and 220 rpm in 250 ml baffled flask
170 for 50 h. 1 ml was harvested from each culture at 13000 x g (Heraeus Fresco 21, Thermo
171 Scientific), 4°C for 2 min. The supernatants were acidified before threefold ethyl acetate
172 extraction as previously described (Purohit et al., 2013). The ethyl acetate phase was dried using
173 rotary vacuum centrifuge (CentriVap, Labconco) at 40°C for 15 min, and then redissolved in 150
174 μ l of 20% acetonitrile containing 0.1% formic acid and 775 nM of the internal standard 3OC12-
175 HSL.

176 *Detection of AHL profiles using a mix of HPLC-MS/MS and full scan HR-MS analysis*

177 The detection of AHL was adapted from the methods described previously (Hansen et al., 2015).
178 Briefly: the samples (20 μ l) were injected onto an Ascentis Express C185 cm x 2.1 mm, 2.7 μ m
179 reverse phase column (Supelco) using an Accela autosampler (Thermo scientific). The elution
180 was performed using an Accela pump (Thermo scientific) with an acetonitrile gradient in 0.1%
181 formic acid, and consisted of 5% acetonitrile for 18 seconds, followed by a linear gradient up to
182 90% acetonitrile over 222 seconds, and finally 90% acetonitrile for 60 seconds. The column was
183 re-equilibrated for 60 seconds with 5% acetonitrile in 0.1% formic acid before the next sample
184 was injected. Flow rate was 500 μ l/min for all steps.

185 The separated compounds were ionized in positive ion electrospray using the following settings:
186 sheath gas flow rate 70, auxiliary gas flow rate 10, sweep gas flow rate 10, spray voltage +4.50
187 kV, capillary temperature 330°C, capillary voltage 37 V, and tube lens 80 V.

188 The ionized components were detected using an LTQ Orbitrap XL (Thermo scientific) run in
189 either ms/ms low resolution mode or full scan HRMS mode. C4 AHL's are difficult to detect
190 using full scan HR-MS analysis due to co-eluting isobaric compounds seen in some samples, so
191 these components together with 3OC6 and 3OHC6 were measured using HPLC MS/MS using
192 the LTQ part of the LTQ orbitrap XL. The rest of the compounds were measured using Full
193 Scan HR-MS analysis. The C4's, 3OHC6 and 3OC6 elute early in the chromatogram, and were
194 measured in 2 segments each with 3 scan events. Segment 1 ran from 0 min to 0.88 min, with the
195 following scan events. m/z 172.10 \rightarrow (101.2-103.2) (C4-HSL), m/z 186.10 \rightarrow (101.2-103.2)
196 (3OC4-HSL) and 188.10 \rightarrow (101.2-103.2) (3OHC4-HSL). Segment 2 ran from 0.88 min to 1.76

197 min with the following scan events: 172.10-> (101.2-102.3) (C4-HSL), 214.10-> (101.2-102.3)
198 (3OC6-HSL), 216.12-> (101.2-102.3) (3OHC6-HSL). Segment 3 ran from 1.76 min to 5 min in
199 which the rest of the compounds were measured using only one scan event, FTMS (165-450)
200 resolution 15000. Target setting was 5×10^5 ions per scan, and maximum injection time was 250
201 ms. Lock mass was enabled for correction of background ions from caffeine (m/z 195.0877) and
202 diisooctyl phthalate (m/z 391.2843 and m/z 413.2662). The system was calibrated with a mixture
203 of 15 AHLs including the internal standard 3OC12-HSL, and the ion chromatograms were
204 analyzed using the Xcalibur v. 2.18 software package. The mass window was set to 8 parts per
205 million. The limit of detection (LOD) and the limit of quantification (LOQ) for the different
206 AHLs were calculated as previously described (Purohit et al., 2013).

207 **Construction of GFP tagged *A. salmonicida* strains**

208 *A. salmonicida* mutants ($\Delta ainS$, *luxI*, $\Delta ainSluxI$ and $\Delta litR$) used in this study were
209 constructed previously (Bjelland et al., 2012; Hansen et al., 2015). The mutants were tagged with
210 GFP using tri-parental mating as described by others. Briefly; the pVSV102 plasmid carrying the
211 gene coding for GFP and kanamycin was transferred from *E. coli* DH5 α pir to the mutant strains
212 using the conjugative helper strain CC118 λ pir harboring pEVS104 helper plasmid. Donor and
213 helper cells were grown to mid-log phase ($OD_{600} = 0.7$) in LB1. Recipient strains (*A.*
214 *salmonicida*) were grown to early stationary phase ($OD_{600} = 1.2$) in LB2.5. The donor, helper
215 and recipient strains were harvested (13000 x g, 1 min) and washed twice with LB1 before they
216 were mixed in 1 to 1 ratio and spotted onto BA2.5 plates, followed by overnight incubation at
217 16°C. The spotted cells were resuspended in LB2.5 and incubated for 24 h. at 12°C with

218 agitation (220 rpm). The potential tagged strains were selected on BA2.5 after 5 days. The
219 tagged strains were confirmed microscopically with Nikon Eclipse TS100.

220 **Static biofilm assay**

221 The biofilm assay was performed as described previously (Hansen et al., 2014; Khider,
222 Willassen & Hansen, 2018). Briefly; the overnight secondary cultures were grown to an OD₆₀₀
223 of 1.3. The secondary cultures were further diluted 1:10 in SWT and a total volume of 300 µl
224 was added to each well in flat-bottom, non-tissue culture-treated Falcon 24-well plates (BD
225 Bioscience). A final concentration of 1400 ng/ml of 3OC6-HSL, 100 ng/ml of 3OHC10-HSL,
226 197 ng/ml of 3OC8, 100 ng/ml of C8 and 400 ng/ml of C6 were added to each well. The plates
227 were incubated statically at 8°C, for 72 h. and the biofilm was visualized using Nikon Eclipse
228 TS100 microscope at 10x magnification and photographed with Nikon DS-5Mc. The biomasses
229 of the biofilms were quantified using crystal violet. The medium was removed and 300 µl of
230 0.1% (wt/vol) crystal violet in H₂O was added. The plates were incubated at room temperature
231 for 30 min. The crystal violet stain was removed by flipping the plates gently, and the wells were
232 washed twice with 0.5 ml of H₂O. The wells were air dried overnight and the biofilm was
233 dissolved in 0.5 ml of 96% ethanol with agitation (250 rpm) overnight. The dissolved biofilm
234 was diluted 1:10 in 96% ethanol and transferred to a 96-well plate (100 µl/well). The absorbance
235 was measured at 590 nm (Vmax kinetic microplate reader; Molecular Devices).

236 **Soft agar motility assay**

237 The motility assay was performed using soft agar plates containing 0.25% agar and 2.5%
238 NaCl as previously described (Khider, Willassen & Hansen, 2018). Briefly; the secondary
239 overnight cultures were diluted to an OD₆₀₀ of 0.4. Then 3 µl of each culture was spotted on the
240 soft agar plates and incubated at 8°C for 5 days. The degree of motility for each strain was
241 monitored every 24 hours for 5 days by measuring the diameters of spreading halos on the soft
242 agar plate.

243 **Colony morphology assay**

244 The colony morphology assay was carried mainly as described before (Hansen et al., 2014;
245 Khider, Willassen & Hansen, 2018). From each secondary overnight culture, a 250 µl was
246 harvested by centrifugation, and the pellet was re-suspended in 250 µl SWT. Then, 2 µl of each
247 culture was spotted onto SWT agar plates, and incubated at 8°C for 14 days. The colonies were
248 viewed microscopically with Zeiss Primo Vert and photographed with AxioCam ERc5s at 4x
249 magnification.

250 **Scanning Electron Microscopy (SEM)**

251 Secondary cultures of *A. salmonicida* strains were grown overnight and fixed with 2.5%
252 (wt/vol) glutaraldehyde and 4% formaldehyde in PHEM-buffer and incubated for one day at 4°C.
253 100 µL of each sample were mounted on a poly-L-lysine coated coverslip for 5 min. Coverslips
254 were washed three times with PHEM buffer before they were postfixed in 1% (wt/vol)
255 Osmiumtetroxide (OsO₄). Samples were further washed for three times with PHEM buffer, all
256 samples were dehydrated with a graded series of ethanol at room temperature for 5 min. The

257 samples were dried using hexamethyldisilazane (HMDS) as a drying agent and further left to dry
258 in a desiccator overnight before being mounted on aluminum stubs, using carbon tape and silver
259 paint. The samples were coated with gold-palladium using a Polaron Range Sputter Coater. Picture
260 were taken with Zeiss Zigma SEM.

261 **Results**

262 **AHL profiling of *A. salmonicida* in SWT medium**

263 In our previous studies, AHL profiling of *A. salmonicida* LFI1238 and mutants thereof were
264 performed after growth in LB2.5 medium. The autoinducer synthase, *AinS* produced one AHL
265 (3OHC10-HSL), and the *LuxI* synthase produced seven AHLs, where the most abundant AHL
266 signal was 3OC6-HSL (Hansen et al., 2015; Purohit et al., 2013). Consequently, when both *luxI*
267 and *ainS* synthases were inactivated, no AHL production was observed in *A. salmonicida* and the
268 double mutant ($\Delta ainSluxI$) produced a biofilm similar to the biofilm of $\Delta litR$ mutant (Hansen et
269 al., 2015). In the work presented here, we wanted to analyze if addition of AHLs could interfere
270 with the biofilm formation of the $\Delta ainSluxI$ double mutant. However, since SWT medium is
271 required for biofilm formation we first wanted to know whether a change of medium would
272 affect the AHLs profiles of *A. salmonicida* wild-type and the mutants.

273 The different *A. salmonicida* strains (LFI1238, $\Delta litR$, $\Delta ainS$, *luxI* and $\Delta ainSluxI$) were grown in
274 SWT medium at 8°C for 50 h. ($OD_{600} \sim 2.0$) before samples were harvested and analyzed using
275 HPLC-MS/MS. The *A. salmonicida* wild-type and mutants showed AHL profiles (Table 2)
276 similar to what have been shown after growth in LB (Hansen et al., 2015) with the exception of
277 C4 and 3OC4. Thus, the wild-type and the $\Delta litR$ AHL profiles consisted of 6 AHLs, where the

278 3OC6-HSL was the most abundant. No AHLs were detected in the *ΔainSluxI* supernatant, the
279 *luxI* mutant produced only 3OHC10-HSL, and the *ΔainS* mutant produced the remaining five
280 AHLs. Compared to the wild-type, the *ΔlitR* mutant produced lower concentrations of the 3OC6-
281 HSL and 3OHC10-HSL confirming that LitR is a positive regulator of these two AHLs also after
282 growth in SWT medium.

283

284 **N-acyl homoserine 3OHC10 and 3OC6 downregulate biofilm formation in *A. salmonicida***

285 To investigate possible effects of 3OC6-HSL (LuxI product) and 3OHC10-HSL (AinS product)
286 on biofilm formation the different AHLs were added to the SWT medium, and *A. salmonicida*
287 strains were allowed to form biofilm at 8°C for 72 h. As shown in Figure 1A, the biofilm
288 formation of *ΔainSluxI* was totally inhibited when supplemented with either 3OHC10-HSL or
289 3OC6-HSL. The *ΔainS*, *luxI* and the wild-type do not form a biofilm (Hansen et al., 2015), and
290 no difference in biofilm formation was found when treated with 3OHC10-HSL or 3OC6-HSL
291 (Figure 1A). The mushroom structured *ΔlitR* biofilm remained unchanged after the addition of
292 AHLs. This shows that LuxI-3OC6-HSL and AinS-3OHC10-HSL functions through LitR, and
293 downregulation on the biofilm formation can not be achieved when *litR* is inactivated (Figure.
294 1A). The addition of C6, C8, and 3OC8 AHLs did not interfere with the biofilm formation of any
295 of the *A. salmonicida* strains (data not shown). Next, the biomasses of treated and untreated
296 biofilms were quantified using crystal violet. Relative to the untreated control samples, the
297 addition of either 3OHC10-HSL or 3OC6-HSL, significantly decreased the biomass of
298 *ΔainSluxI* biofilm (p-value < 0.05). Quantitation of treated and untreated *ΔlitR*, LFI1238, *ΔainS*
299 and *luxI* had no significant differences (Figure 1B). These observations suggest that these two

300 AHLs (3OHC10-HSL and 3OC6-HSL) inhibit biofilm formation in *A. salmonicida* and are
301 operated *via* LitR.

302 ***luxI* mutant forms wrinkled colonies in *A. salmonicida***

303 To determine whether any of the *A. salmonicida* QS systems (*lux* or/and *ain*) are involved in
304 wrinkled colony formation, the *luxI*, Δ *ainS* and the double mutant Δ *ainSluxI* were allowed to
305 form colonies on SWT plates at 8°C. As shown in Figure 2, the Δ *ainS* mutant formed smooth
306 colonies indistinguishable from those formed by the wild-type. This indicates that *ainS* is not
307 required for formation of rugosity. Whereas the *luxI* and Δ *ainSluxI* mutants formed wrinkled
308 colonies similar to the Δ *litR* after 14 days of incubation.

309 **Expression profiles of *A. salmonicida luxI* and Δ *ainS* mutants revealed genes related to QS**

310 In order to gain a better understanding of how LuxI and AinS work in the QS system, the
311 transcriptome expression profiles of *luxI* and Δ *ainS* mutants were compared to the *A.*
312 *salmonicida* LFI1238 wild-type. The expression profiling of *luxI* mutant relative to the wild-type
313 LFI1238 revealed 494 and 446 DEGs at low and high cell densities, respectively, that fell into
314 various functional gene classes adapted from MultiFun (Serres & Riley, 2000) (Figure 3).
315 Among the DEGs at low cell density (LCD) 366 were downregulated and 128 were upregulated
316 (Table S1). Whereas, at high cell density (HCD) 224 genes were downregulated and 222 genes
317 were upregulated (Table S2). Among the upregulated genes that fell into *surface structures*
318 functional group we identified genes of the *tad* operon, which is believed to be associated with
319 adhesion, *VSAL_I10366* (83.8-fold change at LCD and 151.5-fold change at HCD) and

320 *VSAL_H0377* (57.3-fold change at LCD and 39.5-fold change at HCD) coding for fimbrial
321 proteins, Flp/Fap pilin component and type IV leader peptidase, respectively. The remaining
322 genes of the *tad* operon were also upregulated in the *luxI* mutant relative to the wild-type at both
323 cell densities, and are listed in details in the supplementary material (Table S1 and Table S2).

324 As described in our results presented above, the *luxI* mutant formed wrinkled colony
325 morphology on SWT plates. The rugosity is associated with the enhanced production of
326 exopolysaccharides (EPS), which requires the expression of *syp* operon (18 genes) in *A.*
327 *salmonicida* (Hansen et al., 2014; Khider, Willassen & Hansen, 2018). Consistently, our RNA-
328 Seq data at HCD demonstrated 11 significantly upregulated genes of the *syp* operon with fold
329 change values ranging from 9.55 to 2.04.

330 For several bacteria, QS regulates motility and flagellar synthesis (Kim et al., 2007; Ng &
331 Bassler, 2009). Within the *cell processes* functional group, the transcriptome of *luxI* mutant
332 revealed genes associated with motility and chemotaxis (59 DEGs at LCD and 57 DEGs at
333 HCD) (Table S1 and Table S2). The greatest transcript abundance at LCD and HCD were genes
334 encoding sigma 54-dependent transcription regulator, *flrA* and *flrC* in addition to the two-
335 component system *flrB*. Other genes coding for flagellin subunits and flagellar basal body rod,
336 ring, hook and cap proteins, were also downregulated in the *luxI* mutant relative to the wild-type
337 at both cell densities. Additionally, genes coding for methyl-accepting chemotaxis proteins and
338 motor proteins as MotA and MotB were downregulated in the *luxI* mutant.

339 The transcriptome of *ΔainS* revealed fewer genes compared to the *luxI*. Our results presented
340 here show that at LCD we were able to determine a total of 20 DEGs (8 up- and 12

341 downregulated) and at HCD we were able to identify 29 DEGs where 8 were upregulated and 21
342 genes were downregulated (Table S3 and Table S4). The DEGs fell into 10 functional groups
343 (Figure S1). At LCD and in the absence of AHLs, *ain* system act as kinase and serve as
344 phosphoryl-donors to LuxU, which in turn phosphorylates LuxO (Freeman & Bassler, 1999).
345 The $\Delta ainS$ transcriptome demonstrates an upregulation in genes responsible for phosphorylation.
346 The DEGs with high expression level relative to the wild-type was phosphorelay proreïn LuxU
347 (*VSAL_I1875*) with a fold change values of 2.22 and 2.37 at low and high cell densities,
348 respectively. Among the upregulated genes that fell into the *surface structures* functional group
349 we were able to identify genes of the *tad* operon, *VSAL_I10366* gene coding for fimbrial protein
350 with a fold change values of 2.82 and 4.24 at LCD and HCD, respectively. *VSAL_I10367* coding
351 for Flp/Fap pilin component and type IV leader peptidase was identified among upregulated
352 genes at LCD only (Table S3). Among the 21 downregulated genes at HCD our data revealed
353 DEGs with highest fold change to be allocated into *amino acid biosynthesis* as sulfate
354 adenytransferase subunit 1 and 2 encoded by *VSAL_I0421* and *VSAL_I0420*, respectively (Table
355 S4).

356 **LuxI controls motility in *A. salmonicida* LFI1238**

357 The flagellum is required for motility of bacteria, mediating their movements towards favorable
358 environments and avoiding unfavorable conditions (Utada et al. 2014; Zhu, Kojima & Homma,
359 2013). Because the transcriptome results demonstrated that a large panel of flagellar biosynthesis
360 and assembly genes are regulated by *lux* system, we wished to analyze the motility behavior of
361 QS mutants (*luxI*, $\Delta ainS$ and $\Delta ainSluxI$), using soft motility assay.

362 We show that inactivation of *luxI* resulted in a non-motile strain, where the size of the spotted
363 colony (2.0 mm) did not change, indicating no migration from the site of inoculation (Figure
364 4AB). *AinS* was shown to negatively regulate motility in *A. fischeri* (Lupp & Ruby, 2004), and
365 similarly, we assessed the impact of *ainS* deletion on motility of *A. salmonicida*. Compared to
366 the wild-type, which showed motility zones of 26.6 ± 0.57 mm, the Δ *ainS* showed an increased
367 motility, where migration through the soft agar resulted in motility zones of 30.3 ± 0.57 mm. The
368 Δ *ainSluxI* double mutant also demonstrated an increase motility compared to the wild-type with
369 motility zones of 31.3 ± 1.15 mm. (Table S5). In order to determine whether the strains analyzed
370 by soft motility assay possess or lack flagella, the wild-type and the constructed mutants were
371 visualized by SEM. The Δ *ainS* and Δ *ainSluxI* mutants produced several flagella similar to the
372 wild-type. As expected the *luxI* mutant that showed a motility defect, lack flagella in all
373 replicates (Figure 4C).

374 Discussion

375 AHLs have been identified in many vibrio and aliivibrio species including *A. salmonicida*
376 (Buchholtz et al., 2006; Garcia-Aljaro et al., 2008; Purohit et al., 2013; Valiente et al., 2009),
377 which showed to produce a broad range of AHLs through LuxI and *AinS* synthases (Hansen et
378 al., 2015). However, there is still limited understanding of the biological advantages of this AHL
379 diversity in the QS mechanism. In this study, we have demonstrated the influence of *luxI* and
380 *ainS* on the global gene regulation and the impact of AHLs on several phenotypic traits related to
381 QS in order to reveal some answers on the complex network of signal production and regulation
382 in *A. salmonicida*.

383 The ability to form rugose colonies and biofilm are often correlated features in vibrios (Casper-
384 Lindley & Yildiz, 2004; Yildiz & Schoolnik, 1999; Yildiz et al., 2004), where wrinkled colony
385 phenotype is generally associated with enhanced exopolysaccharide production (Yildiz &
386 Schoolnik, 1999). Likewise, in *A. salmonicida* colony wrinkling (rugosity) and biofilm formation
387 requires the expression of *syp* genes responsible for the production of EPS (Hansen et al., 2014;
388 Khider, Willassen & Hansen, 2018). In the study presented here we show that *luxI* mutant
389 exhibited a strong wrinkling colony morphology, indicating an enhanced polysaccharide
390 production. This finding is further confirmed by the transcription analysis, which revealed
391 upregulation of 11 *syp* genes and downregulation of the in the *rpoQ* gene in the *luxI* mutant
392 relative to the wild-type. The sigma factor RpoQ is known to be a strong repressor of *syp* in *A.*
393 *salmonicida* (Khider, Willassen & Hansen, 2018). Earlier studies demonstrated that inactivation
394 of the AHL synthase (e.g *luxI* homologous) in several bacteria caused a reduction in both AHL
395 and EPS production (Koutsoudis et al., 2006; Molina et al., 2005; Von Bodman, Bauer & Coplin,
396 2003). However, here we show that inactivation of *luxI* in *A. salmonicida*, enhanced the EPS
397 production and resulted in wrinkled colonies. Unlike the *luxI* mutants, the *ΔainS* mutant formed
398 smooth colonies, similar to the wild-type and did not show any differentially expressed genes
399 associated with EPS production in the transcriptomics profiling. This indicates that LuxI-derived
400 AHLs are involved in the repression of *syp* genes, where this repression is most likely operated
401 through RpoQ, independent of AinS and the 3OHC10-HSL production.

402 LitR was suggested to link AinS/R and LuxS/PQ systems to LuxI/R systems in *A. salmonicida*,
403 where its deletion influenced the production of AinS and LuxI AHLs. When both *luxI* and *ainS*
404 were inactivated simultaneously, biofilm and colony morphology similar to *ΔlitR* was formed
405 (Hansen et al., 2015). A simple explanation for this observation is the deficiency in AHL

406 production, leading to *litR* inactivation (also *litR* knockout) (Hansen et al., 2014; Bjelland et al.,
407 2012), and thereby no repression on biofilm or colony rugosity is achieved. Furthermore, the
408 exogenous addition of either 3OHC10-HSL (*AinS* signal) or 3OC6-HSL (*LuxI* signal) to
409 $\Delta ainSluxI$, completely inhibited biofilm formation. We have previously shown that the
410 disruption of either EPS or other matrix components (e.g proteins, lipoproteins and eDNA),
411 disrupts the mature biofilm formation in *A. salmonicida* (Hansen et al., 2014; Khider, Willassen
412 & Hansen, 2018). While $\Delta ainS$ mutant did not produce neither mature biofilm nor wrinkled
413 colonies, introduction of *luxI* mutation into $\Delta ainS$, resulted in strains ($\Delta ainSluxI$) with three-
414 dimensional biofilm architecture and wrinkled colonies. These data suggest that these two
415 systems regulate biofilm formation synergistically, where the effect of *AinS* and *LuxI* AHLs is
416 operated through a common pathway as previously reported (Hansen et al., 2015). The results
417 presented here show that both systems function to allow or repress production of EPS and other
418 matrix components. However, the *lux* system is believed to be essential for the production of
419 EPS rather than the *ain* system (discussed above). Studies showed that one key function of EPS
420 involves the attachment of cells to different substratum, which is the initial step in biofilm
421 formation (Vu et al., 2009). For example in *V. cholera*, EPS production is the first step in biofilm
422 formation as cells switch from motile planktonic state to being non-motile and surface attached
423 (Silva & Benitez, 2016). Likewise, we suggest that the non-motile *luxI* mutant, increases EPS
424 production to mediate the initial steps in biofilm formation, whereas *ainS* is neither fully
425 activated nor required at this time. This suggests that *lux* system may operate at a lower threshold
426 cell density than *ain* system, which is more essential at later stages of biofilm development,
427 mainly the maturation into three-dimensional mushroom structure. With our results we expand
428 the previously suggested model, to include *luxI* and *ainS* and their proposed role in regulating

429 biofilm formation and colony rugosity. In the model presented in Figure 5, we propose that as
430 cell density rises 3OHC10-HSL binds AinR receptor, resulting in activation of LitR, which in
431 turn regulates the production of AinS AHL. The activated LitR leads to a repression on other
432 matrix components required for building a mature biofilm as well as activating *rpoQ* resulting in
433 repression of *syp* genes. The *luxI* was proposed to be activated by both LitR and LuxRs. The
434 active LuxI synthesizes seven AHLs and represses *syp* operon via RpoQ. In summary, our results
435 provide clear evidence that the biofilm formation is a low cell density dependent phenotype,
436 when neither LuxI nor AinS AHLs are present. As AHLs accumulate at high cell densities the
437 biofilm is dispersed, indicating that AHL-mediated QS in *A. salmonicida* is involved in the
438 dispersal step of the biofilm cycle.

439 Several bacteria are known to regulate motility via QS, where motility is either activated or
440 inhibited by AHLs (Atkinson et al., 2006; Hoang, Gurich & Gonzalez, 2008; Hussain et al.,
441 2008; Kim et al., 2007; Quinones, Dulla & Lindow, 2005). In the sponge-associated bacteria
442 KLH11 flagellar motility was abolished in the *ssaI* and *ssaR* mutants homologous of *luxI* and
443 *luxR*, respectively (Zan et al., 2012). Similarly, inactivation of *luxI* in *A. salmonicida* led to loss
444 of flagella and motility under our experimental conditions (Figure 4). Consistent with these
445 results, the most pronounced regulation in the *luxI* transcriptome data was observed for genes
446 involved in motility and chemotaxis, exhibiting a significantly low expression level. The motility
447 regulatory cascade has not been well elucidated in *A. salmonicida*, however the motility genes
448 are organized in a similar fashion to *A. fischeri* (Karlsen et al., 2008). Flagellar genes are often
449 grouped into different hierarchical classes; early, middle and late genes, where each class encode
450 genes responsible for entire motility regulon, structural components of the hook-basal body,
451 flagellar filaments, chemotaxis and motor force, respectively (Aldridge & Hughes, 2002). Our

452 results demonstrate DEGs that fell into all classes and thus it is unclear into which regulatory
453 level LuxI affects motility genes. This defect in motility, observed by *luxI*⁻, can not be explained
454 by differences in growth rate, as cultures for different mutants reached the stationary phase
455 (Figure S2). Hence, our observations indicate that LuxI is a positive regulator and required for
456 full motility in *A. salmonicida*, suggesting that the defect in motility is most likely due to impact
457 of LuxI-derived AHLs on the flagellar apparatus. LitR has been shown to be a positive regulator
458 of *ainS* (Hansen et al., 2015). Thus, not surprisingly, we found that Δ *ainS* displayed an increased
459 motility compared to the wild-type, similar to what was reported for Δ *litR* (Bjelland et al., 2012).
460 However, the regulation of motility in *A. salmonicida* and the target of these regulators remain to
461 be determined.

462 We have previously shown that changes in media composition altered biological traits as biofilm
463 formation and colony rugosity in *A. salmonicida* (Hansen et al., 2014). Contrary to what was
464 previously reported (Hansen et al., 2015; Purohit et al., 2013) neither C4-HSL nor 3OC4-HSL
465 were detected in the present work, suggesting that the concentration of these AHLs are either
466 below the detectable limit or not produced due to different culturing temperatures and/or media.
467 However, the profile for the remaining AHLs was unaffected.

468 **Conclusion**

469 In this study we have shown that *luxI* but not *ainS* is essential for formation of wrinkled colonies
470 at low cell density, whereas both systems are required to form a three-dimensional mature
471 biofilm in *A. salmonicida* LFI1238. We also demonstrated that addition of either LuxI-3OC6-
472 HSL or AinS-3OHC10-HSL is able to inhibit the biofilm formation. Our results show that *lux*

473 and *ain* systems regulates biofilm formation through a common pathway, where LuxI acts
474 mainly as a repressor of EPS production (*syp* operon) via RpoQ. While AinS is probably
475 involved in the repression of other matrix components required to build the mature biofilm.
476 Furthermore, we identified differentially expressed genes associated with motility to be regulated
477 by LuxI. These results add a new knowledge to the QS mechanism of *A. salmonicida*, however
478 further investigations are needed to understand the regulation and complexity of this mechanism.

479 **Abbreviation**

480 **AHL:** Acyl homoserine lactone; **GFP:** Green fluorescent protein; **rpm:** rounds per minute;
481 **RNA:** Ribonucleic acid; **tRNA:** transfer RNA; **rRNA:** ribosomal RNA; **h:** hours; **OD:** optical
482 density; **RNA-Seq:** RNA sequencing.

483 **References:**

484 Abisado RG, Benomar S, Klaus JR, Dandekar AA, Chandler JR. 2018. Bacterial Quorum
485 Sensing and Microbial Community Interactions. *MBio* 9
486
487 Aldridge P, Hughes KT. 2002. Regulation of flagellar assembly. *Current Opinion in*
488 *Microbiology* 5:160-165
489
490 Atkinson S, Chang CY, Sockett RE, Camara M, Williams P. 2006. Quorum sensing in *Yersinia*
491 *enterocolitica* controls swimming and swarming motility. *Journal of Bacteriology* 188:1451-
492 1461
493
494 Bjelland AM, Sørnum H, Tegegne DA, Winther-Larsen HC, Willassen NP, Hansen H. 2012. LitR
495 of *Vibrio salmonicida* is a salinity-sensitive quorum-sensing regulator of phenotypes
496 involved in host interactions and virulence. *Infection and Immunity* 80:1681-1689
497
498 Buchholtz C, Nielsen KF, Milton DL, Larsen JL, Gram L. 2006. Profiling of acylated
499 homoserine lactones of *Vibrio anguillarum* in vitro and in vivo: Influence of growth
500 conditions and serotype. *Systematic and Applied Microbiology* 29:433-445
501

- 502 Casper-Lindley C, Yildiz FH. 2004. VpsT is a transcriptional regulator required for
503 expression of *vps* biosynthesis genes and the development of rugose colonial morphology
504 in *Vibrio cholerae* O1 El Tor. *Journal of Bacteriology* 186:1574-1578
505
- 506 Dunn, AK, Millikan DS, Adin DM, Bose JL, Stabb EV. 2006. New *rfp*- and pES213-derived
507 tools for analyzing symbiotic *Vibrio fischeri* reveal patterns of infection and *lux* expression
508 *in situ*. *Applied and Environmental Microbiology* 72: 802-810
509
- 510 Eberhard A, Burlingame AL, Eberhard C, Kenyon GL, Nealon KH, Oppenheimer NJ. 1981.
511 Structural identification of autoinducer of *Photobacterium fischeri* luciferase. *Biochemistry*
512 20:2444-2449
513
- 514 Egidius E, Andersen K, Clausen E, Raa J. 1981. Cold-water vibriosis or "Hitra disease" in
515 Norwegian salmonid farming. *Journal of Fish Diseases* 4:353-354
516
- 517 Egidius E, Wiik R, Andersen K, Hoof KA, Hjeltnes B. 1986. *Vibrio salmonicida* sp. nov., a new
518 fish pathogen. *International Journal of Systematic Bacteriology* 36: 518-520
519
- 520 Emerenini BO, Hense BA, Kuttler C, Eberl HJ. 2015. A Mathematical Model of Quorum
521 Sensing Induced Biofilm Detachment. *PLoS One* 10:e0132385
522
- 523 Fazli M, Almblad H, Rybtke ML, Givskov M, Eberl L, Tolker-Nielsen T. 2014. Regulation of
524 biofilm formation in *Pseudomonas* and *Burkholderia* species. *Environmental Microbiology*
525 16:1961-1981
526
- 527 Fidopiastis PM, Sørum H, Ruby EG. 1999. Cryptic luminescence in the cold-water fish
528 pathogen *Vibrio salmonicida*. *Archives of Microbiology* 171:205-209
529
- 530 Freeman JA, Bassler BL. 1999. A genetic analysis of the function of LuxO, a two-component
531 response regulator involved in quorum sensing in *Vibrio harveyi*. *Molecular Microbiology*
532 31:665-677
533
- 534 Fuqua C, Parsek MR, Greenberg EP. 2001. Regulation of gene expression by cell-to-cell
535 communication: acyl-homoserine lactone quorum sensing. *Annual Review of Genetics*
536 35:439-468
537
- 538 Garcia-Aljaro C, Eberl L, Riedel K, Blanch AR. 2008. Detection of quorum-sensing-related
539 molecules in *Vibrio scophthalmi*. *BMC Microbiology* 8:138
540
- 541 Guvener ZT, McCarter LL. 2003. Multiple regulators control capsular polysaccharide
542 production in *Vibrio parahaemolyticus*. *Journal of Bacteriology* 185:5431-5441
543
- 544 Hansen H, Bjelland AM, Ronessen M, Robertsen E, Willassen NP. 2014. LitR is a repressor of
545 *syp* genes and has a temperature-sensitive regulatory effect on biofilm formation and
546 colony morphology in *Vibrio (Aliivibrio) salmonicida*. *Applied and Environmental*
547 *Microbiology* 80:5530-5541

548

549 Hansen H, Purohit AA, Leiros HK, Johansen JA, Kellermann SJ, Bjelland AM, Willassen NP.
550 2015. The autoinducer synthases LuxI and AinS are responsible for temperature-
551 dependent AHL production in the fish pathogen *Aliivibrio salmonicida*. *BMC Microbiology*
552 15:69

553

554 Hjerde E, Lorentzen MS, Holden MT, Seeger K, Paulsen S, Bason N, Churcher C, Harris D,
555 Norbertczak H, Quail MA, Sanders S, Thurston S, Parkhill J, Willassen NP, Thomson NR.
556 2008. The genome sequence of the fish pathogen *Aliivibrio salmonicida* strain LFI1238
557 shows extensive evidence of gene decay. *BMC Genomics* 9:616

558

559 Hmelo LR. 2017. Quorum Sensing in Marine Microbial Environments. *Annual Review of*
560 *Marine Science* 9:257-281

561

562 Hoang HH, Gurich N, Gonzalez JE. 2008. Regulation of motility by the ExpR/Sin quorum-
563 sensing system in *Sinorhizobium meliloti*. *Journal of Bacteriology* 190: 861-871

564

565 Holm KO, Strøm E, Stensvaag K, Raa J, Jorgensen T. 1985. Characteristics of a *Vibrio* sp.
566 Associated with the "Hitra Disease" of Atlantic Salmon in Norwegian Fish Farms. *Fish*
567 *Pathology* 20:125-129

568

569 Huber B, Riedel K, Hentzer M, Heydorn A, Gotschlich A, Givskov M, Molin S, Eberl L. 2001.
570 The *cep* quorum-sensing system of *Burkholderia cepacia* H111 controls biofilm formation
571 and swarming motility. *Microbiology* 147:2517-2528

572

573 Hussain MB, Zhang HB, Xu JL, Liu Q, Jiang Z, Zhang LH. 2008. The acyl-homoserine lactone-
574 type quorum-sensing system modulates cell motility and virulence of *Erwinia chrysanthemi*
575 *pv. zea*. *Journal of Bacteriology* 190:1045-1053

576

577 Karlsen C, Paulsen SM, Tunsjo HS, Krinner S, Sørum H, Haugen P, Willassen NP. 2008.
578 Motility and flagellin gene expression in the fish pathogen *Vibrio salmonicida*: effects of
579 salinity and temperature. *Microbial Pathogenesis* 45:
580 258-264

581

582 Khider M, Willassen NP, Hansen H. 2018. The alternative sigma factor RpoQ regulates
583 colony morphology, biofilm formation and motility in the fish pathogen *Aliivibrio*
584 *salmonicida*. *BMC Microbiology* 18:116

585

586 Kim J, Kang Y, Choi O, Jeong Y, Jeong JE, Lim JY, Kim M, Moon JS, Suga H, Hwang I. 2007.
587 Regulation of polar flagellum genes is mediated by quorum sensing and FlhDC in
588 *Burkholderia glumae*. *Molecular Microbiology* 64:165-179

589

590 Koutsoudis MD, Tsaltas D, Minogue TD, von Bodman SB. 2006. Quorum-sensing regulation
591 governs bacterial adhesion, biofilm development, and host colonization in *Pantoea*
592 *stewartii* subspecies *stewartii*. *Proceedings of the National Academy of Sciences of the United*
593 *States of America* 103:5983-5988

594

595 Lee KJ, Kim JA, Hwang W, Park SJ, Lee KH. 2013. Role of capsular polysaccharide (CPS) in
596 biofilm formation and regulation of CPS production by quorum-sensing in *Vibrio vulnificus*.
597 *Molecular Microbiology* 90:841-857

598

599 Love MI, Huber W, Anders S. 2014. Moderated estimation of fold change and dispersion for
600 RNA-seq data with DESeq2. *Genome Biology* 15:550

601

602 Lupp C, Ruby EG. 2004. *Vibrio fischeri* LuxS and AinS: comparative study of two signal
603 synthases. *Journal of Bacteriology* 186:3873-3881

604

605 Lupp C, Ruby EG. 2005. *Vibrio fischeri* uses two quorum-sensing systems for the regulation
606 of early and late colonization factors. *Journal of Bacteriology* 187: 3620-3629

607

608 Lupp C, Urbanowski M, Greenberg EP, Ruby EG. 2003. The *Vibrio fischeri* quorum-sensing
609 systems *ain* and *lux* sequentially induce luminescence gene expression and are important
610 for persistence in the squid host. *Molecular Microbiology* 50:319-331

611

612 Magoc T, Wood D, Salzberg SL. 2013. EDGE-pro: Estimated Degree of Gene Expression in
613 Prokaryotic Genomes. *Evololutionary Bioinformatics Online* 9:127-136

614

615 McCarter LL. 1998. OpaR, a homolog of *Vibrio harveyi* LuxR, controls opacity of *Vibrio*
616 *parahaemolyticus*. *Journal of Bacteriology* 180:3166-3173

617

618 Molina L, Rezzonico F, Defago G, Duffy B. 2005. Autoinduction in *Erwinia amylovora*:
619 evidence of an acyl-homoserine lactone signal in the fire blight pathogen. *Journal of*
620 *Bacteriology* 187:3206-3213

621

622 Nelson EJ, Tunsjo SH, Fidopiastis PM, Sørnum H, Ruby EG. 2007. A novel *lux* operon in the
623 cryptically bioluminescent fish pathogen *Vibrio salmonicida* is associated with virulence.
624 *Applied and Environmental Microbiology* 73:1825-1833

625

626 Ng WL, Bassler BL. 2009. Bacterial quorum-sensing network architectures. *Annual Review*
627 *of Genetics* 43:197-222

628

629 Pratt LA, Kolter R. 1998. Genetic analysis of *Escherichia coli* biofilm formation: roles of
630 flagella, motility, chemotaxis and type I pili. *Molecular Microbiology* 30: 285-293

631

632 Purohit AA, Johansen JA, Hansen H, Leiros KH, Kashulin A, Karlsen C, Smalås A, Haugen P,
633 Willassen NP. 2013. Presence of acyl-homoserine lactones in 57 members of the
634 *Vibrionaceae* family. *Journal of Applied Microbiology* 115:835-847

635

636 Quinones B, Dulla G, Lindow SE. 2005. Quorum sensing regulates exopolysaccharide
637 production, motility, and virulence in *Pseudomonas syringae*. *Molecular Plant-Microbe*
638 *Interaction* 18:682-693

639

- 640 Ruby EG, Lee KH. 1998. The *Vibrio fischeri*-*Euprymna scolopes* Light Organ Association:
641 Current Ecological Paradigms. *Applied and Environmental Microbiology* 64:805-812
642
- 643 Serres MH, Riley M. 2000. MultiFun, a multifunctional classification scheme for *Escherichia*
644 *coli* K-12 gene products. *Microbial & Comparative Genomics* 5:205-222
645
- 646 Silva AJ, Benitez JA. 2016. *Vibrio cholerae* Biofilms and Cholera Pathogenesis. *PLoS*
647 *Neglected Tropical Diseases* 10: e0004330
648
- 649 Stabb EV, Ruby EG. 2002. RP4-based plasmids for conjugation between *Escherichia coli* and
650 members of the *Vibrionaceae*. *Methods in Enzymology* 358: 413-426.
651
- 652 Swift S, Downie JA, Whitehead NA, Barnard MA, Salmond PG, Williams P. 2001. Quorum
653 sensing as a population-density-dependent determinant of bacterial physiology. *Advanced*
654 *in Microbial Physiology* 45:199-270
655
- 656 Utada AS, Bennett RR, Fong JCN, Gibiansky ML, Yildiz FH, Golestanian R, Wong GCL. 2014.
657 *Vibrio cholerae* use pili and flagella synergistically to effect motility switching and
658 conditional surface attachment. *Nature Communications* 5:4913
659
- 660 Valiente E, Bruhn JB, Nielsen KF, Larsen JL, Roig FJ, Gram L, Amaro C. 2009. *Vibrio vulnificus*
661 produces quorum sensing signals of the AHL-class. *FEMS Microbiology Ecology* 69:16-26
662
- 663 Verma SC, Miyashiro T. 2013. Quorum sensing in the squid-*Vibrio* symbiosis. *International*
664 *Journal of Molecular Sciences* 14:16386-16401
665
- 666 Von Bodman SB, Bauer WD, Coplin DL. 2003. Quorum sensing in plant-pathogenic bacteria.
667 *Annual Review of Phytopathology* 41:455-482
668
- 669 Vu B, Chen M, Crawford RJ, Ivanova EP. 2009. Bacterial extracellular polysaccharides
670 involved in biofilm formation. *Molecules* 14:2535-2554
671
- 672 Whitehead NA, Barnard AM, Slater H, Simpson NJ, Salmond GP. 2001. Quorum-sensing in
673 Gram-negative bacteria. *FEMS Microbiology Reviews* 25:365-404
674
- 675 Yildiz FH, Liu XS, Heydorn A, Schoolnik GK. 2004. Molecular analysis of rugosity in a *Vibrio*
676 *cholerae* O1 El Tor phase variant. *Molecular Microbiology* 53:497-515
677
- 678 Yildiz FH, Schoolnik GK. 1999. *Vibrio cholerae* O1 El Tor: identification of a gene cluster
679 required for the rugose colony type, exopolysaccharide production, chlorine resistance, and
680 biofilm formation. *Proceedings of the National Academy of Sciences of the United States of*
681 *America* 96:4028-4033
682
- 683 Yildiz FH, Visick KL. 2009. *Vibrio* biofilms: so much the same yet so different. *Trends*
684 *Microbiology* 17:109-118
685

686 Zan J, Cicirelli EM, Mohamed NM, Sibhatu H, Kroll S, Choi O, Uhlson CL, Wysoczynski CL,
687 Murphy RC, Churchill ME, Hill RT, Fuqua C. 2012. A complex LuxR-LuxI type quorum
688 sensing network in a roseobacterial marine sponge symbiont activates flagellar motility
689 and inhibits biofilm formation. *Molecular Microbiology* 85:916-933

690
691 Zhu J, Mekalanos JJ. 2003. Quorum sensing-dependent biofilms enhance colonization in
692 *Vibrio cholerae*. *Developmental Cell* 5:647-656

693
694 Zhu S, Kojima S, Homma M. 2013. Structure, gene regulation and environmental response
695 of flagella in *Vibrio*. *Frontiers in Microbiology* 4:410

696

Table 1 (on next page)

Bacterial strains and plasmids used in this study

1

Bacterial strains or plasmids	Description	Source
<i>A. salmonicida</i>		
LF11238	Wild-type, isolated from Atlantic cod	(Hjerde et al., 2008)
$\Delta litR$	LF11238 containing an in-frame deletion in <i>litR</i>	(Bjelland et al., 2012)
$\Delta ainS$	LF11238 containing an in-frame deletion in <i>ainS</i>	(Hansen et al., 2015)
<i>luxI</i> ⁻	LF11238 containing an insertional disruption in <i>luxI</i> , Cm ^r	(Hansen et al., 2015)
$\Delta ainSluxI$	$\Delta ainS$ containing an insertional disruption in <i>luxI</i> , Cm ^r	(Hansen et al., 2015)
LF11238-pVSV102	<i>A. salmonicida</i> LF11238 carrying pVSV102, Kn ^r	(Khider, Willassen & Hansen, 2018)
$\Delta litR$ -pVSV102	$\Delta litR$ carrying pVSV102, Kn ^r	(Khider, Willassen & Hansen, 2018)
$\Delta ainS$ -pVSV102	$\Delta ainS$ carrying pVSV102, Kn ^r	This study
<i>luxI</i> ⁻ -pVSV102	<i>luxI</i> ⁻ carrying pVSV102, Kn ^r	This study
$\Delta ainSluxI$ -pVSV102	$\Delta ainS luxI$ ⁻ carrying pVSV102, Kn ^r	This study
<i>E. coli</i>		
C118 λ pir	Helper strain containing pEVS104	(Dunn et al., 2006)
DH5 α pir	<i>E. coli</i> strain containing GFP plasmid pVSV102	(Dunn et al., 2006)
Plasmids		
pVSV102	pES213, constitutive GFP, Kn ^r	(Dunn et al., 2006)
pEVS104	R6Korigin, RP4, <i>oriT</i> , <i>trb tra</i> and Kn ^r	(Stabb & Ruby, 2002)

2

3

Table 2 (on next page)

AHL production in *A. salmonicida* LFI1238, $\Delta litR$, $luxI^-$, $\Delta ainS$ and $\Delta ainSluxI^-$.

The values represent the mean of two biological replicates \pm standard deviation.

1

Strains	3OC6 (nM)	C6 (nM)	3OC8 (nM)	3OC10 (nM)	3OHC10 (nM)	C8 (nM)
LF11238	8403 ± 279.3	606 ± 3.5	366 ± 27	67 ± 5.9	161 ± 2.1	28 ± 3.0
<i>Δ<i>litR</i></i>	5173 ± 113.6	593 ± 82.3	330 ± 42.1	72 ± 4.7	11 ± 1.70	25 ± 3.4
<i>luxF</i>	NF	NF	NF	NF	105 ± 6.7	NF
<i>Δ<i>ainS</i></i>	8691 ± 0.0	709 ± 54.6	382 ± 42.5	89 ± 16.9	NF	30 ± 0.0
<i>Δ<i>ainLuxF</i></i>	NF	NF	NF	NF	NF	NF

2

3

4

5

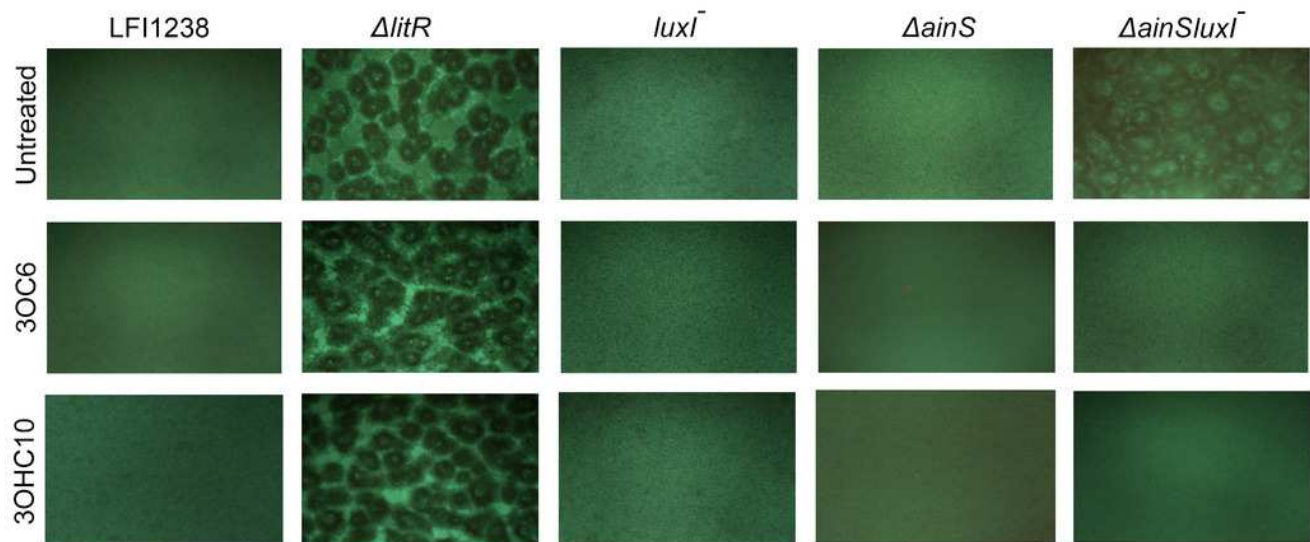
- C4-HSL and 3OC4 were not detected in this analysis
- NF: not found

Figure 1

The effect of 3OC6-HSL and 3OHC10-HSL on biofilm formation of LFI1238, $\Delta litR$, $luxI$, $\Delta ainS$ and $\Delta ainSluxI$.

(A) The strains (LFI1238, $\Delta litR$, $luxI$, $\Delta ainS$ and $\Delta ainSluxI$) were allowed to form biofilm in SWT media supplemented with 1400 ng/ml 3OC6-HSL or 100 ng/ml 3OHC10-HSL at 8°C for 72 h. The biofilms were viewed in a Nikon Eclipse TS100 microscope at 10x magnification and photographed with Nikon DS-5Mc. **(B)** The formed biofilms were staining with crystal violet and quantified by measuring the absorbance at 590 nm. The error bars represent the standard deviation of biological triplicates. (*) represents p-value < 0.05.

A



B

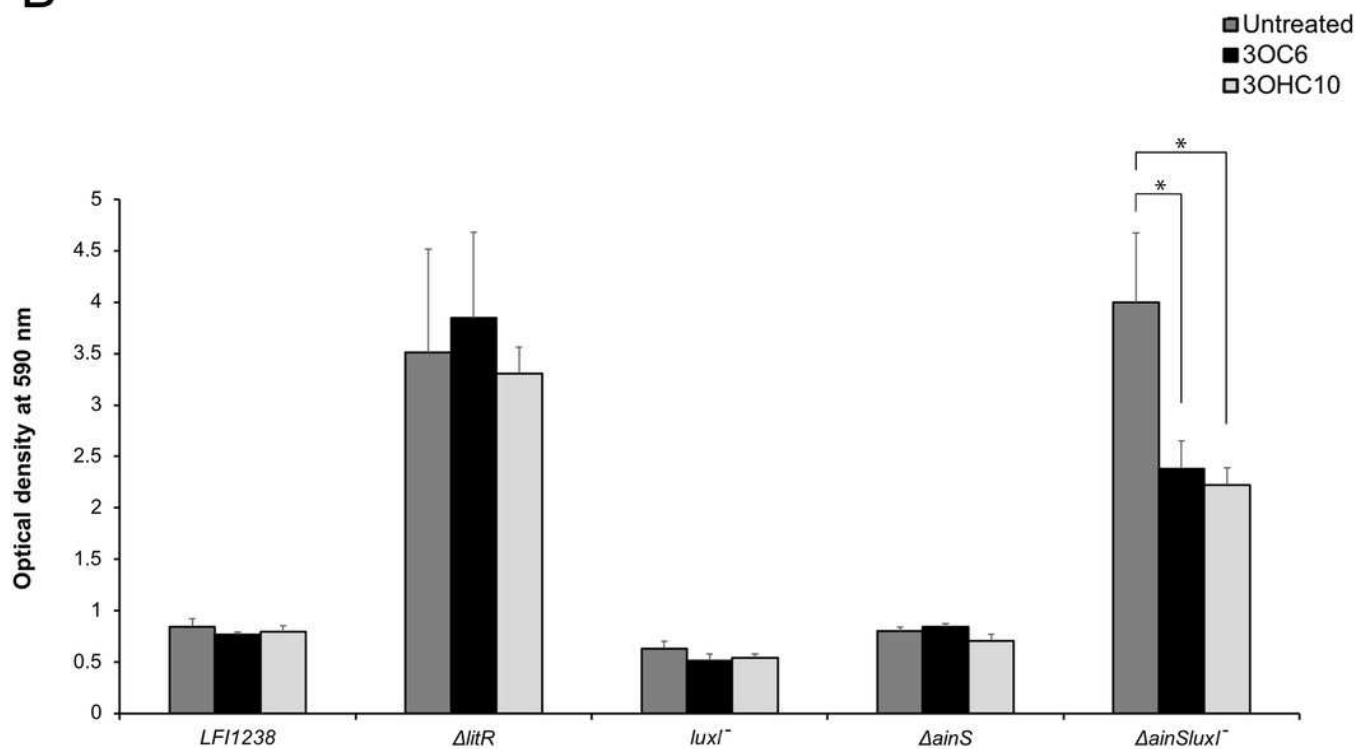


Figure 2

Colony morphology of LFI1238, $\Delta litR$, $luxI$, $\Delta ainS$ and $\Delta ainSluxI$.

The colonies of different strains were allowed to form on SWT plates at 8°C for 14 days. The colonies were viewed in a Zeiss Primo Vert microscope at 4x magnification and photographed with AxioCam ERc5s. Scale bars represent 0.5 mm.

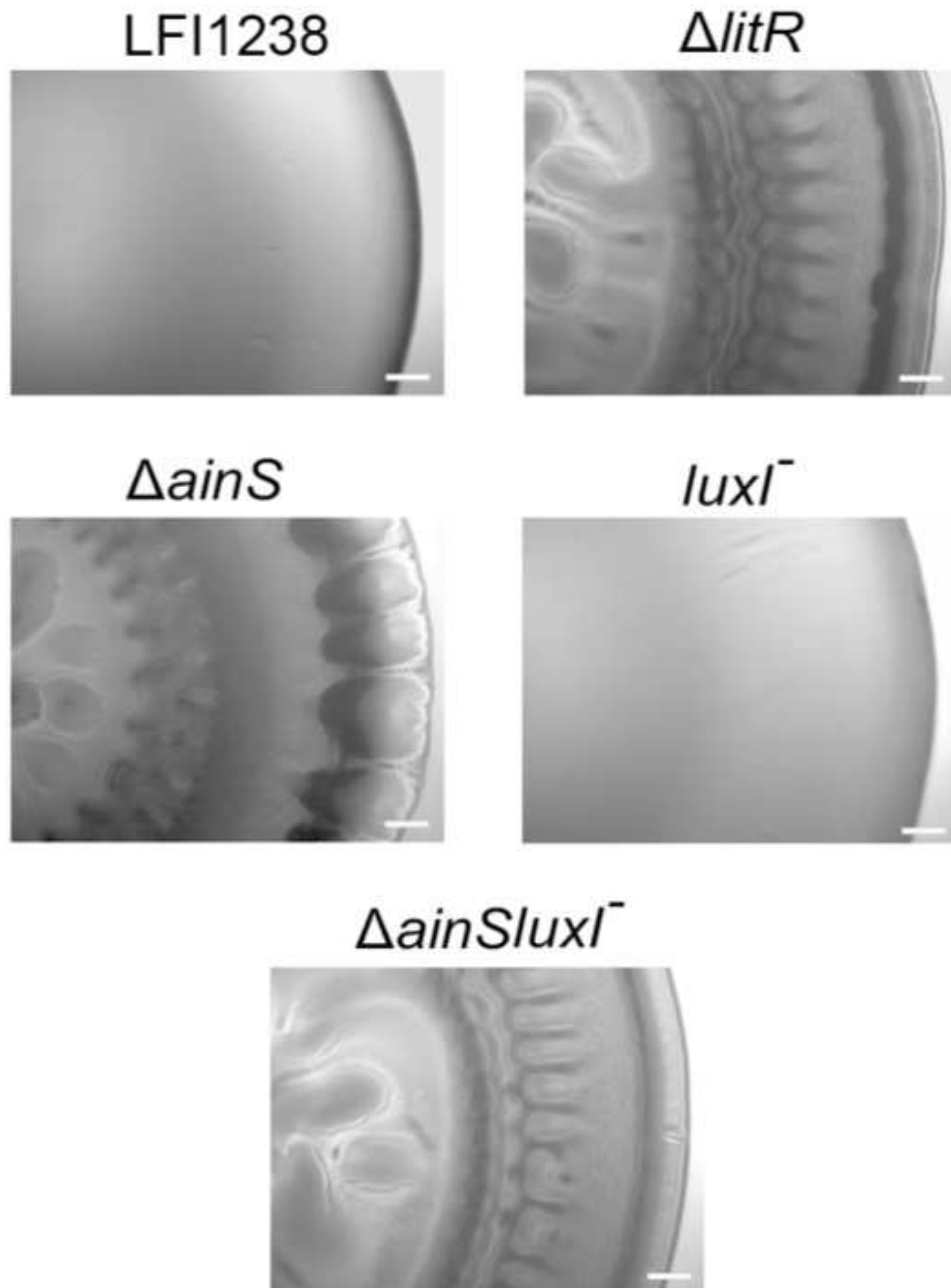


Figure 3

Functional distribution of genes between *A. salmonicida* wild-type and *luxI* mutant at HCD and LCD that are $\geq 2 \times$ differentially expressed.

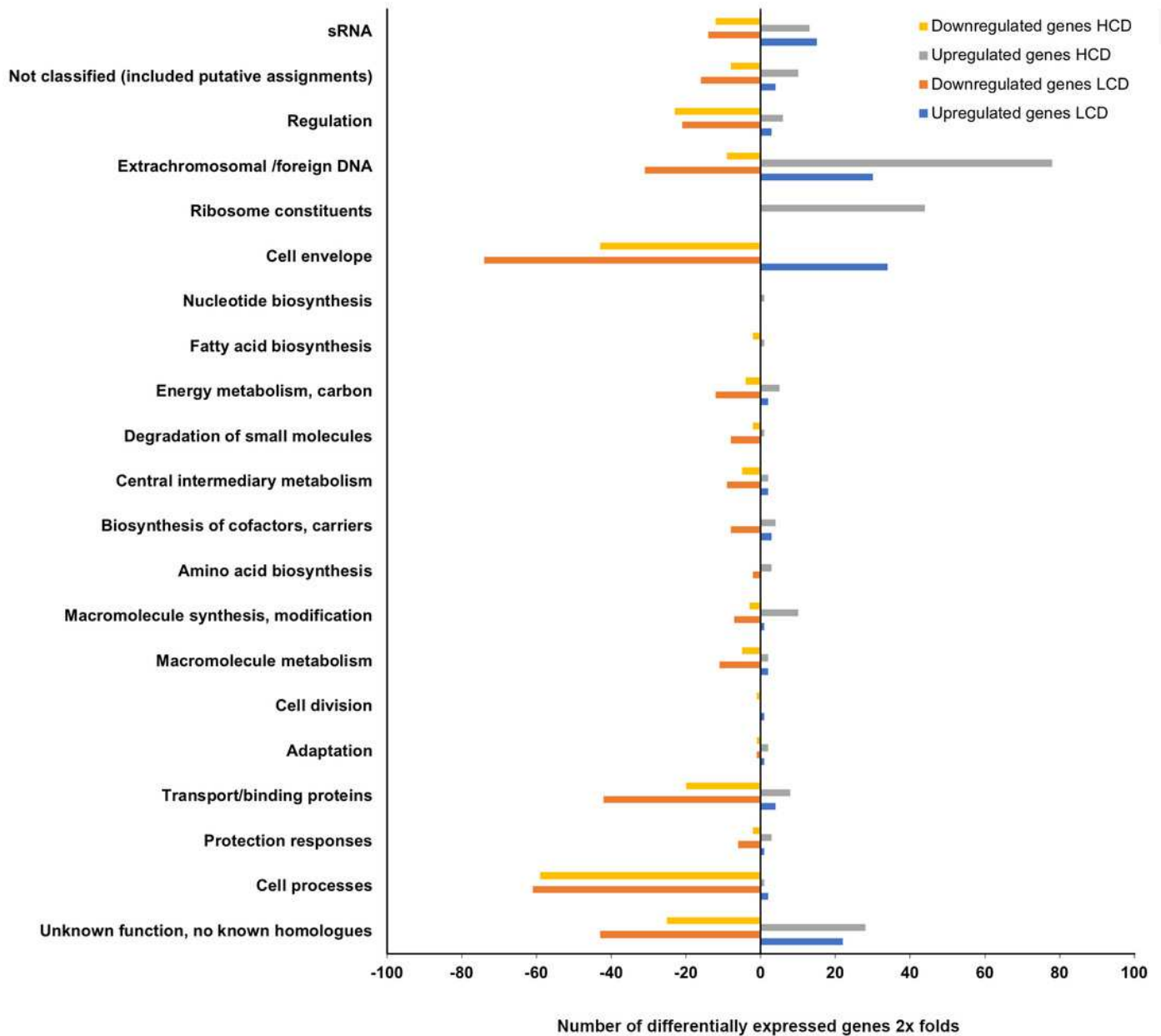


Figure 4

Motility of LFI1238, *luxI*, Δ *ainS* and Δ *ainSluxI*.

(A) Motility zones on soft agar plates after 5 days on incubation at 8°C. **(B)** Measurement of motility zones (mm) of LFI1238, *luxI*, Δ *ainS* and Δ *ainSluxI* after 5 days, error bars are standard deviation of biological triplicates. **(C)** SEM images for flagellum observation of LFI1238, *luxI*, Δ *ainS* and Δ *ainSluxI* taken with Zeiss Zigma at 2kV with an in-lens detector. Scale bars represent 1 mm.

**Note: Auto Gamma Correction was used for the image. This only affects the reviewing manuscript. See original source image if needed for review.*

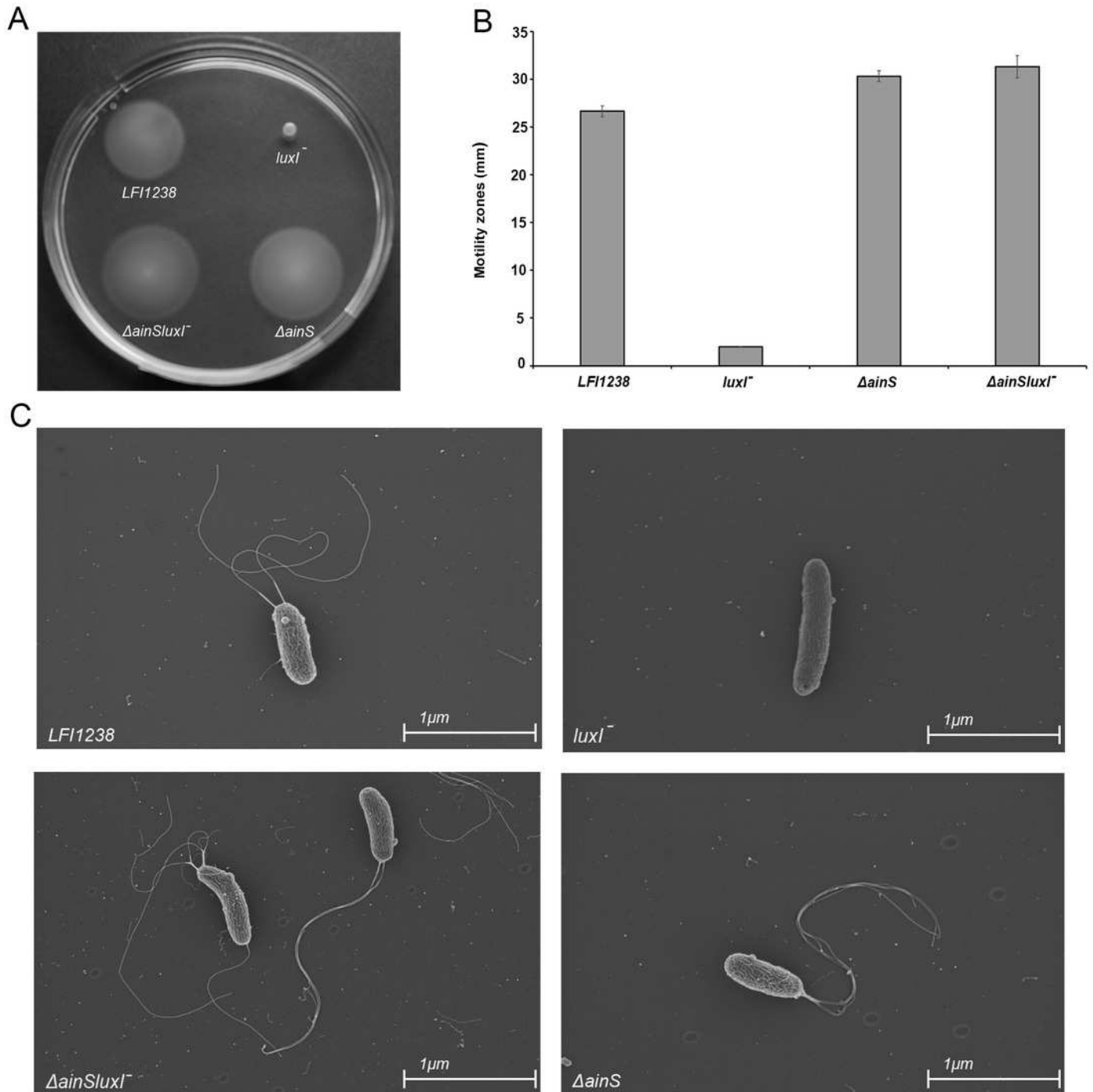


Figure 5

The proposed model of QS system in *A. salmonicida* LFI1238.

The autoinducer synthases LuxI and AinS produce eight AHLs that are transported across the outer (OM) and inner membrane (IM) (Hansen et al., 2015). At high cell density these AHLs are accumulated to reach a critical concentration to be sensed by their receptors (AinR or LuxRs). The AinS-3OHC10-HSL binds AinR, which in turn induces a dephosphorylation cascade, resulting in LitR activation. The expressed LitR, activates the production of the AinS AHL (3OHC10) and the expression of downstream *rpoQ* gene. The increased RpoQ levels represses the *syp* operon leading to biofilm disruption and inhibition of colony rugosity. Moreover, LitR represses other matrix components, through a pathway that remain unknown (Khider, Willassen & Hansen, 2018). LitR together with LuxRs are proposed to regulate *luxI*. The expressed LuxI mediate the production of seven AHLs and represses the *syp* genes via RpoQ. Blue arrows and red lines with bar end indicate pathways of positive and negative regulation, respectively, and may consist of several steps. The thicker, empty arrows indicate the resulting phenotypes.

